

Effects of Nitrogen on Microstructure, Mechanical Properties and Corrosion Behavior in Nickel-Free Austenitic Stainless Steels

S.M. Salehi^{1*} Sh. Kheirandish² S.M. Abbasi³

1- Introduction

Nickel containing austenitic stainless steels can cause inflation and allergic reactions due to releasing nickel ion in the corrosion products. Due to this fact, nitrogen containing nickel-free austenitic stainless steels were substituted with common stainless steels in biomedical applications. Balachandran et al. have reported that every 0.05% of nitrogen is equivalent to 1% nickel for austenite stabilization. It was also reported that the minimum nitrogen which is needed for full austenitic structure is:

$$[\%N]_{\min} = -0.88(\text{wt}\%C) + 0.046(\text{wt}\%Cr) - 0.0009(\text{wt}\%Mn) + 0.038(\text{wt}\%Mo) - 0.053(\text{wt}\%Si) + 0.082(\text{wt}\%Ni) - 0.208(\text{wt}\%Cu) - 0.032(\text{wt}\%W) - 0.278 \quad (1)$$

A recently high nitrogen, manganese austenitic stainless steel (P558) was developed which showed high strength and hardness in solution annealed condition. Carpenter Technology corporation has announced the new high nitrogen steel (with 0.9%wt nitrogen) which has 606MPa yield strength in solution annealed condition which is almost twice the amount of 316L austenitic stainless steel. Generally, nitrogen improves the austenitic stainless steels properties such as: increasing mechanical properties without affecting ductility and toughness, significantly improving corrosion resistance, decreasing the tendency to form strain induced martensite. Thus, the main idea of this research is to find out the effect of nitrogen content on microstructure, mechanical properties and corrosion behavior of nickel-free austenitic stainless steels.

2- Experimental

High nitrogen austenitic stainless steel (HNS) and low nitrogen stainless steel (LNS) were prepared in form of ingots, by melting pure iron and ferroalloys (Cr, Mo, Mn, nitrided ferrochrome, etc.) in appropriate proportions in an induction arc melting furnace. Pure nitrogen gas was used as protective gas. Cast ingots were re-melted by ESR process with CaF₂ and Al₂O₃ slags and it was done under flow of nitrogen gas. The chemical composition of stainless steels is shown in Table 1.

These ingots were solutionized at 1100 °C for 1 hour to remove segregation, and hot-rolled at 1200 °C to reduced thickness. Then they were solution treated at 1100 °C for 1 hour and quenched in water. Samples for microstructure analysis were prepared using manual grinding, and etched by Glyceregia (15ml

HCl+5 ml HNO₃+10 ml Glycerol). The microstructure was studied by optical microscopy.

Tensile test was done according to ASTM E8, using Instron universal testing machine at a strain rate of 2.0 mm/min to determine yield strength (YS), tensile strength (TS), uniform elongation (UE) and total elongation (TE). XRD test was used to identify present phases, using XPert Pro MPD PANalytical with CuK α source. Macrohardness was measured by a Vickers Hardness tester at 30 kg load. The electrochemical tests were performed using a standard three-electrode cell assembly. Saturated calomel electrodes and platinum wire were used as reference and counter electrodes, respectively. The electrolyte solution used in this test was 200 ml of Ringer solution. The experiments were carried out using IVIUMSTAT with IviumSoft software for simulating EIS and Potentiodynamic polarization data. EIS measurements were performed in the frequency range from 10 mHz to 100kHz. Potentiodynamic polarization experiments were carried out by changing the electrode potential from -250mV to 2V at a scan rate of 0.001 V/s. The corrosion current density (i_{corr}), corrosion potential (E_{corr}), corrosion rate and other parameters were automatically extracted from the polarization curves by the Tafel extrapolation.

3-Results and Discussion

Fig. 1 shows the microstructure of HNS (Fig. 1a) and LNS (Fig. 1b) which reveals fully austenitic grains with average size of 20 \pm 5 μ m for HNS, and austenite-ferrite grains with average ferrite size of 25 \pm 5 μ m and average austenite size of 8 \pm 3 μ m for LNS. Fig. 1 also shows the annealing twins in austenite grains, which caused to decrease grain boundary energy.

According to Eq. (1) and Table 1, the minimum required nitrogen for fully austenite structure is 0.5 wt.% for HNS. However, LNS, which didn't have this minimum amount, has austenite-ferrite structure. Fig. 2 illustrates the X-ray diffraction profiles of annealed samples at room temperature. XRD investigations exposed only the presence of peaks corresponding to austenite in HNS as well as austenite and ferrite in LNS and no evidences for formation of martensite or any other phase.

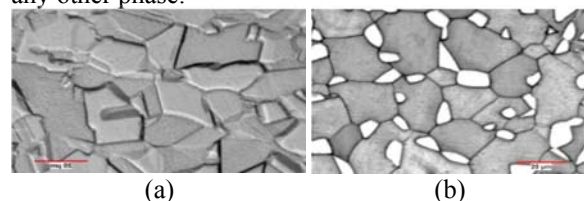


Fig. 1 Optical micrographs of (a) HNS: fully austenite grains with annealing twins and (b) LNS: microstructure of austenite (bright phase) and ferrite (dark phase) in annealed condition

^{1*} Corresponding Author, M.Sc. School of Metallurgy and Materials Engineering, Iran University of Science and Technology. Email: s_ms5@yahoo.com

² Professor, School of Metallurgy and Materials Engineering, Iran University of Science and Technology, Tehran, Iran.

³ Associate Professor, Metallic Materials Research Center (MMRC), Maleke Ashtar University of Technology, Tehran, Iran.

Table 1 Chemical composition of stainless steels

Sample	C	Cr	Mn	Mo	Si	S	P	N	Fe
HNS	0.04	19.8	22.1	1.40	1.41	0.03	0.003	1.1	Bal.
LNS	0.04	19.7	21.9	1.38	1.38	0.02	0.003	0.03	Bal.

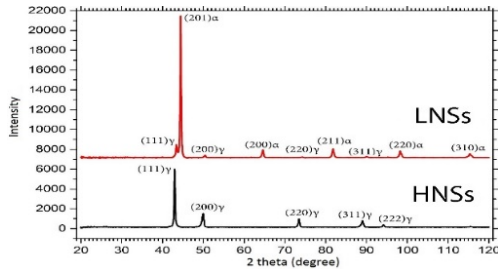


Fig. 2 XRD patterns of annealed HNS and LNS

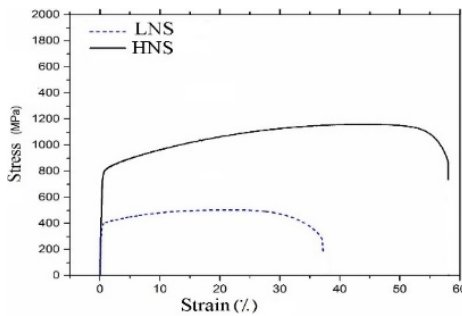


Fig. 3 Stress-strain curves of annealed HNS and LNS

Table 2 Tensile properties and hardness of annealed samples

Sample	YS(MPa)	TE(MPa)	UE (%)	TE (%)	Hardness (Hv)
HNS	790	1160	43	57	331
LNS	387	503	23	37	206

Fig. 4 shows the polarization curves of stainless steel sample in Ringer's solution at 37 °C. The figure shows that the polarization current was low before the pitting occurs and then the current increased to a high level. Polarization parameters were obtained from the extrapolation of the polarization curve for the stainless steels and their values are recorded in Table 3.

It may be seen that the values of corrosion current density (i_{corr}) decreased with increasing nitrogen content. While the corrosion potential (E_{corr}) and linear polarization resistance (LPR) increase with increasing nitrogen content. The breakdown potential (E_{bd}) is another important parameter in selecting material for biomedical applications. E_{bd} in HNS is significantly more than that of LNS.

Impedance spectra was used for evaluating passive film stability on the samples' surface after passive film had formed. Fig. 5 shows the Nyquist curve of HNS and LNS at 37 °C in Ringer's solution. The values of electrochemical impedance parameters are presented in Table 4. It was observed that the corrosion resistance of HNS is more than LNS.

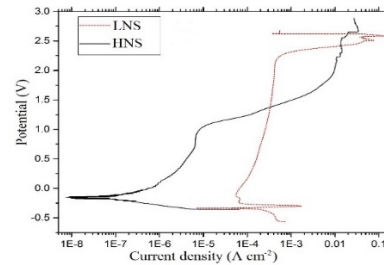


Fig. 4 Polarization curves in Ringer's solution at 37 °C for HNS and LNS.

Table 3 Polarization parameters for different stainless steels in Ringer's solution at 37 °C

Samples	E_{corr} (V)	i_{corr} ($\mu\text{A}/\text{cm}^2$)	C.Rate (mm/y)	LPR (Ω)	E_{bd} (V)
HNS	-0.1463	0.0316	0.000371	2.64×10^6	1.15
LNS	-0.3737	0.277	0.003256	1.356×10^5	-0.21

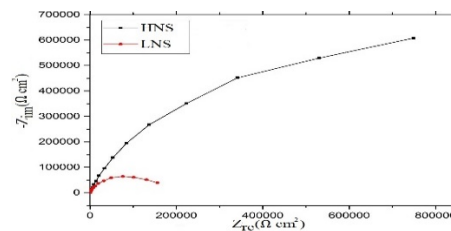


Fig. 5 Nyquist plot of HNS and LNS in Ringer's solution at 37 °C

Table 4 EIS parameters for HNS and LNS in Ringer's solution at 37 °C

Samples	Rct (Ω)	CPE (F/cm^2)	n
HNS	1.6×10^6	4.016×10^{-7}	0.811
LNS	1.783×10^5	1.45×10^{-6}	0.8292

4- Conclusions

The following conclusions can be drawn from the present study:

Microstructure of HNS is fully austenitic with the presence of annealing twins. Although, the microstructure of LNS is austenite + ferrite. Strain-induced martensite and secondary phases were not observed in either microstructure.

Yield strength and tensile strength were increased with increasing nitrogen content without considerably decreasing elongation. Besides, the addition of nitrogen increases the hardness of samples significantly.

Nitrogen content showed a significant influence on the corrosion behavior of SS. The corrosion rates decreased with increasing nitrogen content in the alloy.